



**HAL**  
open science

## Root functional traits determine the magnitude of the rhizosphere priming effect among eight tree species

Lin Chao, Yanyan Liu, Weidong Zhang, Qingkui Wang, Xin Guan, Qingpeng Yang, Longchi Chen, Jianbing Zhang, Baoqing Hu, Zhanfeng Liu, et al.

### ► To cite this version:

Lin Chao, Yanyan Liu, Weidong Zhang, Qingkui Wang, Xin Guan, et al.. Root functional traits determine the magnitude of the rhizosphere priming effect among eight tree species. *Oikos*, 2023, pp.e09638. 10.1111/oik.09638 . hal-03986265

**HAL Id: hal-03986265**

**<https://hal.science/hal-03986265>**

Submitted on 13 Feb 2023

**HAL** is a multi-disciplinary open access archive for the deposit and dissemination of scientific research documents, whether they are published or not. The documents may come from teaching and research institutions in France or abroad, or from public or private research centers.

L'archive ouverte pluridisciplinaire **HAL**, est destinée au dépôt et à la diffusion de documents scientifiques de niveau recherche, publiés ou non, émanant des établissements d'enseignement et de recherche français ou étrangers, des laboratoires publics ou privés.

1 **Root functional traits determine the magnitude of the rhizosphere priming effect**  
2 **among eight tree species**

3

4 Lin Chao<sup>1,2,3</sup>, Yanyan Liu<sup>2</sup>, Weidong Zhang<sup>1,4,\*</sup>, Qingkui Wang<sup>1,4</sup>, Xin Guan<sup>1,4</sup>,  
5 Qingpeng Yang<sup>1,4</sup>, Longchi Chen<sup>1,4</sup>, Jianbing Zhang<sup>2</sup>, Baoqing Hu<sup>2</sup>, Zhanfeng Liu<sup>5</sup>,  
6 Silong Wang<sup>1,4,\*</sup>, Grégoire T. Freschet<sup>6</sup>

7 <sup>1</sup> Institute of Applied Ecology, Chinese Academy of Sciences, Key Laboratory of  
8 Forest Ecology and Management, Shenyang, 110016, China, <sup>2</sup> Key Laboratory of  
9 Environment Change and Resources Use in Beibu Gulf, Ministry of Education,  
10 Nanning Normal University, Nanning, 530001, China, <sup>3</sup> University of Chinese  
11 Academy of Sciences, Beijing, 100049, China, <sup>4</sup> Huitong Experimental Station of  
12 Forest Ecology, Chinese Academy of Sciences, Huitong, 418307, China, <sup>5</sup> Key  
13 Laboratory of Vegetation Restoration and Management of Degraded Ecosystems &  
14 CAS Engineering Laboratory for Vegetation Ecosystem Restoration on Islands  
15 Coastal Zones, South China Botanical Garden, Chinese Academy of Sciences,  
16 Guangzhou, 510650, China, <sup>6</sup> Station d'Ecologie Théorique et Expérimentale, CNRS,  
17 2 route du CNRS, 09200 Moulis, France

18 \*For correspondence. *Email wdzhang@iae.ac.cn, slwang@iae.ac.cn*

19

20

21 **Abstract**

22 Living roots and their rhizodeposits can accelerate or decelerate the decomposition of  
23 soil organic matter which refers to the rhizosphere priming effect (RPE). However,  
24 whereas plant traits are thought to be key factors controlling the RPE, little is known  
25 about how root traits representative of plant biomass allocation, morphology,  
26 architecture, or physiology influence the magnitude of the RPE. Using a natural  
27 abundance  $^{13}\text{C}$  tracer method allowing partitioning of native soil organic carbon (SOC)  
28 decomposition and plant rhizosphere respiration, we studied here the effects of eight  $\text{C}_3$   
29 tree species featuring contrasting functional traits on  $\text{C}_4$  soil respiration over a 204-day  
30 period in a microcosm experiment. All tree species enhanced the rate of SOC  
31 decomposition, by 82% on average, but the strength of the rhizosphere priming  
32 significantly differed among species. Mean diameter of first-order roots and root  
33 exudate-derived respiration were positively correlated with the RPE, together  
34 explaining a large part of observed variation in the RPE ( $R^2 = 0.72$ ), whereas root  
35 branching density was negatively associated with the RPE. Path analyses further  
36 suggested that mean diameter of first-order roots was the main driver of the RPE owing  
37 to its positive direct effect on the RPE and its indirect effects via root exudate-derived  
38 respiration and root branching density. Our study demonstrates that the magnitude of  
39 the RPE is regulated by complementary aspects of root morphology, architecture and  
40 physiology, implying that comprehensive approaches are needed to reveal the multiple  
41 mechanisms driving plant effects on the RPE. Overall, our results emphasize the  
42 relevance of integrating root traits in biogeochemical cycling models to improve model

43 performance for predicting soil C dynamics.

44 **Keywords:**  $^{13}\text{C}$  natural abundance,  $\text{C}_4$  soil, fine roots, root functional traits, organic

45 matter decomposition, soil organic carbon

46

## 47 **Introduction**

48 Soil organic matter (SOM) represents the largest reservoir of organic carbon (C) in  
49 terrestrial ecosystems, holding approximately 2500 Pg C (up to 1 m depth) (Tifafi et al.  
50 2018). Therefore, even a minor change in soil organic C (SOC) stocks would have  
51 major effects on atmospheric CO<sub>2</sub> concentration and would have potential feedback to  
52 climate (Davidson and Janssens 2006, Heimann and Reichstein 2008, Qiao et al. 2014).  
53 The size of SOC pools is largely determined by the balance between C inputs from plant  
54 production and C outputs from soil decomposers, whereas its stability is reflected in the  
55 microbial mineralization of SOC (Davidson and Janssens 2006, Cotrufo et al. 2015,  
56 Guenet et al. 2018). Soil CO<sub>2</sub> output consists of two distinct components, rhizosphere  
57 respiration by roots and associated microbes utilizing root-derived substrates, and  
58 microbial decomposition of native SOC (Zhu et al. 2014). Historically, soil temperature  
59 and water content have been considered as the primary drivers of SOC decomposition  
60 (Davidson and Janssens 2006). However, emerging evidence indicates that plant roots  
61 and rhizosphere inputs are also major drivers of decomposition processes (Fontaine et  
62 al. 2007, Schmidt et al. 2011, Finzi et al. 2015, Keiluweit et al. 2015). The presence of  
63 live roots can accelerate or decelerate SOC decomposition via the ‘rhizosphere priming  
64 effect’ (RPE, defined as a change in SOC decomposition by the supply of root-derived  
65 substrates). For example, in the presence of living roots, SOC decomposition can  
66 decrease by up to 79% (negative RPE), or increase by as much as 500% (positive RPE),  
67 relative to rootless soil (Cheng et al. 2014, Huo et al. 2017).

68 The magnitude, direction and duration of the RPE can be influenced by multiple

69 factors, including plant species identity (Cheng et al. 2014, Henneron et al. 2019) and  
70 plant traits (e.g. photosynthesis rate, plant biomass and phenology; Yin et al. 2018,  
71 Henneron et al. 2019), and soil properties (e.g. soil type, nutrient availability, soil  
72 temperature and water content; Zhu and Cheng 2011, 2013, Dijkstra et al. 2013).  
73 Several hypotheses have been proposed to explain the underlying mechanisms of  
74 contrasting RPEs. Generally, positive RPEs could be explained by co-metabolism of  
75 SOC with root-released available substrates (i.e. root exudates) that stimulate microbial  
76 growth and extracellular enzyme production (Kuzyakov, 2002; Cheng and Kuzyakov,  
77 2005). Additionally, root exudates may also destabilize mineral-associated organic SOC,  
78 thereby enhancing microbial access to previously mineral-protected compounds  
79 (Keiluweit et al., 2015). By contrast, negative RPEs might occur if microbial  
80 communities switch from degrading recalcitrant SOC to utilizing energy-rich root  
81 exudates (“preferential substrate utilization hypothesis”, Cheng and Kuzyakov, 2005),  
82 or if plants and microorganisms compete for nutrients (“nutrient competition  
83 hypothesis”, Kuzyakov and Xu, 2013; Chang et al. 2020).

84 Over the past decade, many studies have indicated that plant biomass and traits  
85 significantly influence the intensity of the RPE (Cheng et al., 2003; Pausch et al., 2013;  
86 Henneron et al., 2019). Previous studies have demonstrated that plant biomass was  
87 generally positively correlated with RPE, at least for herbaceous species (Dijkstra et al.  
88 2006, Zhu and Cheng 2013, Huo et al. 2017). Furthermore, the magnitude of the RPE  
89 is strongly influenced by the quantity and chemical composition of root exudates  
90 (Cheng et al. 2014, Wang et al. 2016), which are not only regulated by plant biomass

91 (Zhu and Cheng 2013), but also related to some root functional traits (Meier et al. 2020,  
92 Sun et al. 2021). Root traits may indeed be particularly important drivers of the  
93 magnitude and dynamics of the RPE due to their intricate relationship with the soil  
94 matrix and microorganisms (Finzi et al. 2015, Carrillo et al. 2017, Henneron et al. 2019).  
95 Root exudation rate (approximated in the present study by the CO<sub>2</sub> released from root  
96 exudates) is likely to be one of the strongest drivers of the RPE (Shahzad et al. 2015,  
97 Wang et al. 2016). In addition, fine roots with high metabolism (e.g. high respiration  
98 rate; Sun et al. 2021) and large surface of exchange (as represented by fine-root length;  
99 Freschet et al. 2021a) could strongly influence rhizosphere processes by changing  
100 rhizosphere properties (e.g. soil pH, nutrient status, microbial communities; Bais et al.  
101 2006, Freschet et al. 2021b). For example, species with high root length increase the  
102 contact of roots with soil and the input of C to soil (Bardgett et al. 2014). Similarly,  
103 species with a high proportion of root tips (as represented by fine-root branching density,  
104 RBD; Freschet et al. 2021b) could show increased root exudation (mostly located at the  
105 root tips; Canarini et al. 2019). As such, these traits may all be important drivers of the  
106 RPE.

107       Recent studies further suggest that root exudation may be linked to root  
108 morphology, as observed at the intraspecific level between specific root length (SRL)  
109 and root exudation rate (positive relationship; Meier et al. 2020). Negative relationship  
110 of root tissue density (RTD) and root diameter with root exudation rate was also  
111 observed at the interspecific level (Han et al. 2020, Sun et al. 2021). However, the  
112 influence of such traits morphological traits on the RPE is likely to be largely indirect,

113 through covariation of these traits with traits more directly linked to root exudation and  
114 the RPE, for example, root length and root respiration rate (see discussion in Freschet  
115 et al. 2021a). In support for this, several studies showed that root exudation may also  
116 be largely decoupled from both root morphology and mycorrhizal colonization (across  
117 16 crop species; Wen et al. 2019), and that root morphological traits, such as SRL and  
118 diameter, were weak predictors of the RPE (Wang et al. 2016, Henneron et al. 2019).

119 Our understanding of root trait-RPE relationships is currently limited for several  
120 reasons. First, most studies to date on root traits-RPE relationships used a relatively  
121 small pool of species (Cheng et al. 2003, Pausch et al. 2013, Yin et al. 2020, but see  
122 Han et al. 2020). Second, although a meta-analysis can partly solve this problem by  
123 including a large pool of plant species (Huo et al. 2017), the lack of data on root  
124 morphology does not allow us to establish reliable relationships between root  
125 morphological traits and the RPE (Cheng et al. 2014, Huo et al. 2017). Moreover,  
126 studies suggesting an absence of relationship between root morphological traits and the  
127 RPE are based on observations made on herbaceous species only (Henneron et al. 2019,  
128 Wang et al. 2016) and cannot be simply extrapolated to tree species as trait-trait and  
129 trait-function relationships may differ across plant functional types (Freschet et al.  
130 2021a). Interestingly, while, in a study of 14 woody species, Han et al. (2020) observed  
131 that root functional traits such as root diameter strongly correlated with the rhizosphere  
132 effect on SOM decomposition their results included both the effect of rhizodeposits  
133 decomposition and the RPE. Finally, not accounting for trait differences between root  
134 orders may also influence root morphology-RPE relationships (Henneron et al. 2019)

135 as root functions vary along root orders (Freschet and Roumet 2017). Particularly, first-  
136 order roots show high metabolic activity and respiration rate, and host a large part of  
137 root exudation processes (Canarini et al. 2019). Therefore, we differentiated here  
138 between root traits of first-order roots, which we expected to be most strongly related  
139 to root exudation processes, and root traits of absorptive roots.

140 The primary aim of this experiment was to examine the main drivers of root-trait  
141 effect on the RPE. To do so, the isotope-based method was used to determine RPE and  
142 identify its correlation with plant traits across woody species. Specifically, we studied  
143 the  $^{13}\text{C}$  isotopic signature of  $\text{CO}_2$  respired from microcosms where eight  $\text{C}_3$  tree species  
144 from different families were planted in a  $\text{C}_4$  soil. Owing to large species differences in  
145 plant biomass and a range of fine-root morphological, architectural and physiological  
146 traits, we expected that plant species would exert a strong influence on the magnitude  
147 of the RPE. We further expected that the stimulation of SOC decomposition should  
148 depend simultaneously on contrasting aspects of plant functioning, including biomass,  
149 morphology, architecture and physiology. More precisely, we tested the hypotheses that  
150 (i) among a range of tree species, high biomass, fine root length, root branching density,  
151 and root exudation rate would be the main drivers of the RPE; and that (ii) these traits  
152 would have complementary (i.e. non-redundant) effects on the RPE because of their  
153 key role in determining the amount, location and activity of the roots.

154

## 155 **Materials and methods**

### 156 **Experimental setup**

157 The  $^{13}\text{C}$  natural abundance approach was used to separate plant-derived  $\text{CO}_2\text{-C}$  from  
158 soil-derived  $\text{CO}_2\text{-C}$  by planting  $\text{C}_3$  plants in  $\text{C}_4$  soil. The soil used in this study was  
159 collected from the plow layer (0–20 cm) of a farm plot that has been grown with a  $\text{C}_4$   
160 maize crop for over 23 years. The soil was air-dried, thoroughly homogenized and  
161 passed through a 4 mm mesh sieve. The soil is a clay loam (43% sand, 22% silt, 35 %  
162 clay) with a pH of 6.9. The C and nitrogen (N) concentrations were  $17.3 \text{ g kg}^{-1}$  and  $1.5$   
163  $\text{g kg}^{-1}$ , respectively, corresponding to a C:N ratio of 11.6. The  $\delta^{13}\text{C}$  value of  $\text{C}_4$  maize  
164 soil was  $-16.5\%$ .

165 Eight common and relatively abundant tree species in a subtropical forest were  
166 used in this experiment (Table 1). Tree seedlings of similar size (height and diameter  
167 were *c.* 37.8 cm and 5.4 cm) were taken from a common garden and transplanted into  
168 polyvinyl chloride (PVC) pots (diameter 16 cm, height 40 cm), equipped with a PVC  
169 lid at the bottom. A nylon bag filled with 2 kg sand was placed at the bottom of each  
170 pot for drainage, and 6.6 kg air-dried  $\text{C}_4$  soil was packed into each pot at a bulk density  
171 of  $1.27 \text{ g cm}^{-3}$ . Pots without plants were also included as control. There were 45 pots in  
172 total, with five replicates of each species (for *Quercus acutissima*, *Carya cathayensis*  
173 and *Schima superba* only four replicates were available at the end of the experiment,  
174 owing to the death of one tree replicate). We note that a ninth species, *Metasequoia*  
175 *glyptostroboides*, was also planted, but was excluded from this study due to very poor  
176 development during the experiment. The plants were left to grow for 204 days (the  
177 whole growing season, from March to October 2018, with a temperature range of 20.5  
178 to  $31 \text{ }^\circ\text{C}$ ,  $23.8 \text{ }^\circ\text{C}$  on average). The pots were placed under natural conditions located at

179 the Huitong Natural Research Station of Forest Ecosystem (26°48'N, 109°30'E) in the  
180 Hunan province, central China. Local mean annual temperature and precipitation are  
181 16.5 °C and 1200 mm. The soil moisture in each pot was measured gravimetrically and  
182 maintained at 80% of its water holding capacity via regular watering and the use of a  
183 rain shelter to exclude rainfall during rain events.

184

### 185 **Analysis of CO<sub>2</sub> fluxes**

186 We measured the total respiration of the plant-soil system from each pot with an air-  
187 tight, opaque CO<sub>2</sub> chamber trapping system (Figure S1). The dark conditions inside the  
188 chamber prevented photosynthesis and, thereby, the uptake of CO<sub>2</sub> by the plant  
189 (Shahzad et al. 2015). The CO<sub>2</sub> released by the plant-soil systems was quantified by  
190 taking air samples from chambers on day 54, 90, 120 and 204 after planting.  
191 Specifically, two holes were punched on the top of PVC chamber lids and installed with  
192 bulkhead connectors. Polyurethane tubes were used for linking the bulkhead connectors  
193 with a manual valve. Pots were placed inside the PVC chamber (diameter 20 cm, height  
194 100 cm) and the chambers were flushed by circulating air for 5 minutes to ensure a  
195 common CO<sub>2</sub> starting point, using an air compressor. An air sample was taken to  
196 measure the initial CO<sub>2</sub> concentration, then chambers were sealed immediately by  
197 closing the manual valve. After 48 h, the gas was collected using a portable Gas  
198 sampling pump and stored in a pre-evacuated Gas sampling bag, and pots were taken  
199 out of the chamber. Dark incubations of 48 h or less prevent the substantial decrease in  
200 root activity and soil respiration typically observed for longer incubations (Kuzyakov

201 and Cheng 2001). The CO<sub>2</sub> concentration and δ<sup>13</sup>C were analyzed by a High-precision  
202 Isotopic CO<sub>2</sub> Cavity Ring-Down Spectrometer (CRDS) (Picarro G2131-i Analyzer,  
203 Picarro, Inc., Santa Clara, CA, USA). The amount of CO<sub>2</sub> derived from the plant-soil  
204 system respiration and its δ<sup>13</sup>C were obtained by correcting for the initial atmospheric  
205 CO<sub>2</sub> (Wang et al. 2016).

206

### 207 **Harvest and Measurements**

208 The pots were destructively harvested 204 days after the planting of tree seedlings  
209 (Figure S2). Plant shoots were cut off at the base, then the pots were cut into two halves  
210 longitudinally to ensure the structural integrity of root systems. We shook the root  
211 system gently until only well-attached soil remained on the root system and carefully  
212 collected the soil still adhering to the roots (Figure S1), which was defined as  
213 rhizosphere soil (Phillips et al. 2006, Sun et al. 2021). Bulk soil was collected from  
214 unplanted treatment. Rhizosphere and bulk soil respiration were measured during 12 h  
215 incubation at 25 °C (Wang et al. 2016). Briefly, 10 g of soil (either fresh rhizosphere or  
216 bulk) was weighed into a 1 L Mason jar and gas was collected 12 h after sealing using  
217 a portable gas sampling pump and stored in a pre-evacuated gas sampling bag. Previous  
218 results typically assume that the amount of root exudate is proportional to root-derived  
219 CO<sub>2</sub> (Ataka et al., 2020). Another proxy for the amount of root exudate can be measured  
220 as the respired CO<sub>2</sub> derived from rhizosphere soil within a few hours after sampling, as  
221 this respiration should be strongly related to the microbial utilization of root exudates  
222 (Fischer et al., 2010; Wang et al., 2016). Here, we tried to refine these relatively rough

223 proxies to more accurately estimate root exudation. As such, in our study, eight C<sub>3</sub> tree  
224 species were planted in C<sub>4</sub> soil, so we were able to use the <sup>13</sup>C natural tracer approach  
225 to further partition root exudate-derived CO<sub>2</sub> (C<sub>3</sub>-C) from rhizosphere soil-derived CO<sub>2</sub>  
226 (C<sub>4</sub>-C). The CO<sub>2</sub> concentration and δ<sup>13</sup>C value of respired CO<sub>2</sub> were also analyzed by a  
227 High-precision Isotopic CO<sub>2</sub> CRDS, as described above.

228 After harvest, plant roots were gently washed with deionized water to remove  
229 residual soil particles adhering to roots. The root samples were stored in clean plastic  
230 bags and frozen at -20 °C until subsequent morphology and architecture measurements.  
231 Root orders were described and dissected according to stream ordering system, where  
232 the most distal roots are first order and where second-order roots begin at the junction  
233 of two first-order roots and so on (Pregitzer et al. 2002, McCormack et al. 2015). Roots  
234 from each order were scanned in deionized water using a clear water tray at 600 dpi on  
235 a Microtek *i800 plus* scanner and analyzed with WinRhizo (Regent Instruments,  
236 Quebec, Canada). Root length, diameter, and root volume can be directly obtained  
237 through WinRhizo software output. However, root volume was recalculated from the  
238 sum of the volumes of all diameter classes, as the volume provided by Winrhizo is  
239 strongly biased (Freschet et al. 2021a). All plant samples were oven-dried at 65 °C for  
240 3 days to constant weight and weighed.

241 Specific root length was calculated on first-order roots and on absorptive roots (the  
242 first three root branch order following a morphometric classification; McCormack et al.  
243 2015) by dividing the length of these root entities by their oven-dried mass (m g<sup>-1</sup>). For  
244 these same root entities, root tissue density was calculated as the dry mass of root per

245 unit volume of fresh root ( $\text{g cm}^{-3}$ ), root length density was calculated as the length of  
246 root per unit soil volume ( $\text{cm cm}^{-3}$ ). Root branching density was expressed as the  
247 number of first-order laterals per centimeter of second order root ( $\text{cm}^{-1}$ ) to allow for  
248 comparison with the literature (such as Eissenstat et al. 2015). Root exudate-derived  
249 respiration ( $\text{C}_3\text{-C}$ ) was calculated by subtracting the  $\text{CO}_2$  efflux of the rhizospheric soil  
250 ( $\text{C}_4\text{-C}$ ) from the total  $\text{CO}_2$  efflux, as further described below, and was denoted as  $\text{mg C}$   
251  $\text{kg}^{-1} \text{soil d}^{-1}$ .

252

### 253 **Calculations**

254 The total respiration of the plant-soil system was calculated for each pot and  
255 harvest date as follows:

$$256 \quad R_{\text{total}} = \frac{C \times V \times M}{22.4 \times W \times t} / \left( \frac{273}{273 + T} \right)$$

257 where  $R$  is the  $\text{CO}_2$  efflux ( $\mu\text{g C kg}^{-1} \text{soil day}^{-1}$ );  $C$  is the measured  $\text{CO}_2$  concentration  
258 (ppm);  $V$  is the effective volume of a PVC chamber (21.3 L);  $M$  is the molar mass of C  
259 ( $12 \text{ g mol}^{-1}$ );  $W$  is the dry weight of soil (g);  $t$  is the time of  $\text{CO}_2$  accumulation (day);  
260 and  $T$  is the temperature ( $^{\circ}\text{C}$ ) of incubation.

261 We partitioned the total  $\text{CO}_2$  efflux ( $R_{\text{total}}$ ) ( $\text{mg C kg}^{-1} \text{soil d}^{-1}$ ) of the plant-soil  
262 system incubation into SOC decomposition ( $R_{\text{soil}}$ ) and plant-derived  $\text{CO}_2$  ( $R_{\text{plant}}$ ) using  
263 a two-source isotopic mixing-model:

$$264 \quad R_{\text{soil}} = R_{\text{total}} \times \frac{(\delta^{13}\text{C}_{\text{plant}} - \delta^{13}\text{C}_{\text{total}})}{(\delta^{13}\text{C}_{\text{plant}} - \delta^{13}\text{C}_{\text{soil}})}$$

$$265 \quad R_{\text{plant}} = R_{\text{total}} - R_{\text{soil}}$$

266 where  $\delta^{13}\text{C}_{\text{total}}$  and  $\delta^{13}\text{C}_{\text{soil}}$  are  $\delta^{13}\text{C}$  values of  $\text{CO}_2$  emitted from planted and

267 unplanted treatment at each sampling date, respectively, and  $\delta^{13}\text{C}_{\text{plant}}$  is the  $\delta^{13}\text{C}$  value  
268 of root respiration. Previous studies showed that the separation of root- and SOM-  
269 derived  $\text{CO}_2$ , as a prerequisite to calculate RPE, often involves the assumption that the  
270 net isotopic fractionation during respiration processes is negligible (Schnyder and  
271 Lattanzi, 2005; Dijkstra et al., 2010; Henneron et al. 2019). However, isotopic  
272 fractionation between root tissue and root-respired  $\text{CO}_2$  has been increasingly  
273 recognized (Zhu et al., 2011; Yin et al., 2018). Therefore, we used the  $^{13}\text{C}$  value of root  
274 respiration in this study, i.e. we considered the  $\delta^{13}\text{C}$  fractionation between root-derived  
275  $\text{CO}_2\text{-C}$  and root biomass.  $R_{\text{plant}}$  includes both the plant autotrophic respiration and the  
276 respiration of C contained in rhizodeposits by soil micro-organisms. The average  
277  $\delta^{13}\text{C}_{\text{plant}}$  ranged from  $-32.4\text{‰}$  to  $-28.1\text{‰}$  across species (Table S1), with an average  
278 difference of  $13.6\text{‰}$  relative to  $\delta^{13}\text{C}_{\text{soil}}$  ( $-16.5\text{‰}$ ). The RPE was calculated by  
279 subtracting the  $\text{CO}_2$  derived from unplanted soil from the SOM-derived  $\text{CO}_2$  of the  
280 planted soil ( $\text{mg C kg}^{-1} \text{ soil d}^{-1}$ ):

$$281 \text{PRE} = R_{\text{soil(planted)}} - R_{\text{soil(unplanted)}}$$

282 The average daily  $R_{\text{soil}}$ ,  $R_{\text{plant}}$  and  $RPE$  were calculated as the average of all four  
283 sampling dates.

284 Rhizospheric soil respiration ( $R_{\text{rhizospheric soil}}$ ) and root exudate-derived respiration  
285 ( $R_{\text{exudates}}$ ) were further calculated based on the incubation of rhizospheric soil sampled  
286 at the end of the experiment. We partitioned the total  $\text{CO}_2$  efflux ( $R_{\text{sum}}$ ) ( $\text{mg C kg}^{-1} \text{ soil}$   
287  $\text{d}^{-1}$ ) of the rhizospheric soil incubation using a two-source isotopic mixing-model:

$$288 R_{\text{rhizospheric soil}} = R_{\text{sum}} \times \frac{(\delta^{13}\text{C}_{\text{exudates}} - \delta^{13}\text{C}_{\text{sum}})}{(\delta^{13}\text{C}_{\text{exudates}} - \delta^{13}\text{C}_{\text{bulk soil}})}$$

289  $R_{\text{exudates}} = R_{\text{sum}} - R_{\text{rhizospheric soil}}$

290 where  $\delta^{13}\text{C}_{\text{sum}}$  and  $\delta^{13}\text{C}_{\text{bulk soil}}$  are  $\delta^{13}\text{C}$  values of  $\text{CO}_2$  emitted from the incubation of  
291 rhizospheric (planted treatment) and bulk soil (unplanted treatment), respectively;  
292  $\delta^{13}\text{C}_{\text{exudates}}$  is the  $\delta^{13}\text{C}$  value of  $\delta^{13}\text{C}_{\text{root}}$  (‰). Based on a previous study on three tree  
293 species sampled five times along the year (Gougherty et al. 2018), where an average  
294 difference of 1.2‰ was observed between  $\delta^{13}\text{C}_{\text{exudates}}$  and  $\delta^{13}\text{C}_{\text{root}}$ , we conducted a  
295 sensitivity analysis to estimate the consequence of using  $\delta^{13}\text{C}_{\text{root}}$  as a proxy for  
296  $\delta^{13}\text{C}_{\text{exudates}}$  on root-exudate respiration values and relationships between root-exudate  
297 respiration and RPE, and observed a relatively limited impact (Table S2, S3).

298

### 299 **Statistical analysis**

300 To comply with normality and homogeneity assumptions of all parametric tests, root  
301 tissue density, root length and root length density of first-order roots and absorptive  
302 roots were  $\log_{10}$ -transformed. Two-way ANOVA was used to assess the effects of plant  
303 species, sampling time and their interaction on the level of RPE among species. One-  
304 way ANOVA with Tukey's HSD post-hoc tests were further used to compare plant  
305 above and belowground biomass and traits among different species. A correlation  
306 analysis was carried out to test collinearity among all these plant variables (Table S6).  
307 The absence of relationship between plant biomass variables and traits indicated the  
308 likely absence of allometric effects of plant size on trait values. The relationships  
309 between all of these plant variables and the RPE was first tested using univariate linear  
310 regression analyses. Then, a cut-off of  $R^2 > 0.4$  was used to retain variables with highest

311 explanatory power on RPE in univariate regressions (namely, mean diameter of first-  
312 order roots, root branching density and root exudate-derived respiration) and conduct  
313 multivariate regressions. All possible combinations of these retained variables were  
314 used in multiple linear regression models to test their potential to explain the variance  
315 in RPE (no collinearity issue was detected among these variables, with all pairwise  
316 Pearson correlation coefficients  $< 0.6$ ). The best models were selected based on  
317 corrected Akaike information criterion (AICc). Statistical analyses for all data were  
318 carried out using SPSS version 16.0 (SPSS Inc., Chicago, Illinois, USA) and the  
319 significance level was set at  $P < 0.05$ .

320         Additionally, we used path analysis (Shipley 2015) to develop and test hypotheses  
321 regarding the causal relationships between plant traits that showed (marginally-)  
322 significant univariate relationships with the RPE. Our initial hypothesized causal  
323 structure (Figure 4a) generally reflects the idea that plant investment towards first-order  
324 roots (via high root biomass of first-order root and high root branching density) that  
325 increases the presence and distribution of first-order roots highly active in exuding  
326 compounds would stimulate soil carbon priming, as discussed earlier in this manuscript.  
327 The same initial model including traits measured on absorptive roots rather than first-  
328 order roots was also tested. These two versions of the initial model were then strongly  
329 adapted, based on results of univariate relationships between root traits and the RPE to  
330 obtain a final model that successfully accounted for the patterns of conditional  
331 dependencies in the data. Path coefficients that were not statistically different from zero  
332 were removed unless they had clear biological justifications and increased the fit of the

333 model. We maintained two such marginally non-significant path coefficients in the final  
334 model (Figure 4). Acknowledging the poor fit of models including the root length  
335 variable, this variable was replaced by two of its component traits, mean root diameter  
336 and specific root length. We used the 'sem' function in the 'lavaan' package of R  
337 (Rosseel 2012). The data were fitted to the models using the maximum likelihood  
338 estimator with standard errors and Chi-square test statistic. We conducted all statistical  
339 analyses within the R statistical environment (Version 4.0.5, R Core Development Team,  
340 2021-03-31).

341

## 342 **Results**

### 343 **Substantial interspecific variation among plant biomass and root functional traits**

344 The eight species used in this study exhibited a wide range of plant biomass and root  
345 trait values (Table S4). All 19 measured plant characteristics differed significantly  
346 among species ( $P < 0.0001$ , Table 1), except for two, root branching density and  
347 rhizosphere soil respiration. Across the eight species, there was a 3–45-fold variation in  
348 plant biomass, first-order root biomass showed the largest variation (CV= 100.6%),  
349 aboveground biomass had the lowest variation (CV = 40%). Root morphological traits  
350 showed 2–43-fold variation, and ranged from a CV of 27% for first-order root diameter  
351 to a CV of 82% for absorptive specific root length. Root branching density and root  
352 exudate-derived respiration showed similar variation ( $CV_{RBD} = 23.8\%$  vs.  $CV_{root\ exudate} =$   
353 21.9%). Also, a similar range of variation was found for composite (biomass-related)  
354 root traits (coefficient of variation ranging between 137% and 143%). By contrast,

355 rhizosphere soil respiration had the lowest cross-species variation (CV = 5.9%) among  
356 plant biomass and root functional traits.

357

### 358 **CO<sub>2</sub> efflux and primed SOC**

359 The total CO<sub>2</sub> efflux of the plant-soil system showed a similar trend across all eight  
360 species, that is, an initial decrease in soil CO<sub>2</sub> efflux, then an increase up to the  
361 maximum value on day 120, then again a decrease over time (Figure 1). The magnitude  
362 of plant-derived CO<sub>2</sub>, the total CO<sub>2</sub> efflux and primed C were all significantly affected  
363 by sampling time (Table S5). In addition, all of these soil parameters were influenced  
364 by species identity (Table S5).

365 Over the 204 days of plant growth, the eight treatments with plants all exhibited  
366 higher soil CO<sub>2</sub> production relative to the unplanted control. Mean daily CO<sub>2</sub>  
367 production from the unplanted control was 1.08 mg C kg<sup>-1</sup> soil day<sup>-1</sup>, against 2.90 mg  
368 C kg<sup>-1</sup> soil day<sup>-1</sup> on average in planted pots. This ranged from 2.67 (*Schima superba*) to  
369 4.13 mg C kg soil day<sup>-1</sup> (*Cunninghamia lanceolata*) depending on the species (Figure  
370 2a). All species induced a positive RPE, corresponding to an acceleration of SOC  
371 decomposition compared to the unplanted control over the entire experimental period  
372 (Figure 2a). There were significant differences in RPE among species with values  
373 ranging from 0.75 to 1.03 mg C kg soil day<sup>-1</sup> during the entire experimental period  
374 (Figure 2a). The magnitude of RPE was also significantly affected by sampling time  
375 and the interaction between sampling time and plant species (Figure 2b). Over the 204  
376 days of growth, compared to the unplanted treatment, the presence of plants stimulated

377 the decomposition of SOC by 82 % on average, with the lowest for *Triadica sebifera*  
378 (70%) and the highest for *Cunninghamia lanceolata* (96%) (Figure 2b). However, there  
379 was no significant difference in the RPE between ECM and AM tree mycorrhizal type  
380 (Figure S3).

381

### 382 **Plant biomass and root traits as potential drivers of the RPE**

383 Three plant traits, including aspects of root morphology, architecture and physiology  
384 were significantly or marginally-significantly related to the RPE (Table 2; Figure 3).

385 This included positive relationships between the RPE and mean diameter of first-order  
386 roots ( $MRD_{1st}$ ;  $R^2 = 0.61$ ,  $P = 0.02$ ) and root exudate-derived respiration ( $R^2 = 0.42$ ,  $P$   
387  $= 0.08$ ). The RPE was also negatively related to RBD ( $R^2 = 0.52$ ,  $P = 0.04$ ). Interestingly,  
388 there was no relationship between plant growth rate and the PRE ( $R^2 = 0.00$ ,  $P = 0.92$ )  
389 and the type of mycorrhizal association did not influence the RPE ( $P = 0.86$ ).

390 Considering all plant traits together, the combination of  $MRD_{1st}$  and RBD  
391 appeared most relevant to explain the RPE ( $R^2 = 0.72$ ,  $P = 0.043$ ; Table 3). Further, a  
392 path analysis of causal relationships between root traits and the RPE provided a more  
393 detailed picture of potential relationships occurring between root traits and the RPE ( $R^2$   
394  $= 0.79$ ,  $P = 0.947$ , CFI = 1.00, RMSEA = 0.00). This analysis revealed that part of the  
395 relationship between  $MRD_{1st}$  and the RPE was indirect (Figure 4b). The main driver of  
396 RPE was  $MRD_{1st}$  with both a substantial direct effect and indirect effects via its  
397 influence on root exudate-derived respiration, specific root length of first-order roots  
398 ( $SRL_{1st}$ ) and RBD.

399

## 400 **Discussion**

401 The main objective of this study was to investigate how plant traits, with a particular  
402 focus on root traits, affect soil organic carbon decomposition through rhizosphere  
403 priming effects. In contrast with most previous studies, either focusing on grass species  
404 (Shahzad et al. 2015, Wang et al. 2016, Henneron et al. 2019) or on few tree seedlings  
405 (Cheng et al. 2014, Yin et al. 2018, 2020), we used here a relatively larger pool of eight  
406 tree species featuring contrasting functional traits. Our findings provide preliminary  
407 evidence that the magnitude of rhizosphere priming effects is influenced by several root  
408 traits related to aspects of root morphology, architecture and physiology and illustrate  
409 how measuring comprehensive sets of plant traits is necessary to adequately capture the  
410 effects on plants on soil functioning.

411

### 412 **Rhizosphere priming on soil C decomposition**

413 The average stimulation of SOC decomposition by our eight tree species, by 82% on  
414 average, is higher than that the 59% observed by Huo et al. (2017) in a meta-analysis  
415 of 31 studies on RPE, but similar to the 77% recorded for tree species only. Overall, our  
416 and previous results on RPE suggest that RPE may be most positive in the presence of  
417 tree roots as compared to roots of other plant types. However, it remains unclear how  
418 this related to differences in the quantity and quality of root-derived organic matter  
419 between tree and herbaceous species (Wang et al., 2016; Girkin et al., 2018).  
420 Interestingly, this difference may not be simply linked to a difference in mycorrhizal

421 association – trees typically showing either or both of ECM and AM associations as  
422 compared to herbaceous species typically associating with AM fungi only. Indeed,  
423 while previous studies have suggested a potential role of mycorrhiza and the type of  
424 mycorrhizal association in RPE processes (Paterson et al., 2016; Frey 2019, Yin et al.  
425 2021), here we did not observe a difference in RPE between ECM and AM tree  
426 mycorrhizal type. This is despite ECM roots tend to provide more C to the rhizosphere  
427 and have a greater capacity to produce extracellular enzymes than AM roots, suggesting  
428 that ECM roots should typically induce higher RPE than AM roots (Brzostek et al. 2015,  
429 Kumar et al. 2020). Overall, the reasons behind a potentially stronger effect of tree  
430 species on RPE remain uncertain and call for renewed research in this direction.

431 In contrast to the relatively consistent RPE effect observed here among our eight  
432 tree species (from 70% to 96%), other reports of RPE found in the literature present  
433 highly variable values, ranging from a 79% decrease (Thurgood et al. 2014) to an  
434 increase of over 500% in SOC decomposition (Dijkstra and Cheng 2007, Shahzad et al.  
435 2015). Even when considering studies focusing on tree species only the observed  
436 variation in RPE was considerably higher than this observed here. For instance, among  
437 three tree species, Yin et al. (2018) and Bengtson et al. (2012) observed RPE ranging  
438 from 26% to 146%, and from 152% and 244%, respectively. It should be noted that in  
439 the present study the lack of light during the measure of total respiration (48 h) from  
440 plant-soil system, motivated by the need to stop plant absorption of soil respired-CO<sub>2</sub>,  
441 also likely led to an underestimation of the true RPE. During prolonged darkness or  
442 shading, the amount of photosynthates progressively decreases, which negatively

443 affects root exudation, and therefore potentially reduces the magnitude of the RPE as  
444 compared to natural light conditions (Kuzyakov and Cheng 2004, Tang et al. 2019). For  
445 example, the magnitude of the RPE under 40% of ambient full light was only 71% that  
446 observed under full light (Chang et al. 2020). Besides, there is some evidence that the  
447 effect of light intensity may be further modulated by plant species identity and traits (Li  
448 et al. 2020). Additionally, our method also likely slightly underestimates the true RPE  
449 due to its inability to detect primed C of very old organic matter dating from before the  
450 23 years of C<sub>4</sub> plant cultivation.

451 We found that the magnitude of RPE was significantly affected by the sampling  
452 time, in line with previous studies (Zhu et al., 2011; Wang et al., 2016; Wang et al.,  
453 2020). However, the lack of destructive sampling at different stages does not allow to  
454 explore how the dynamics of plant above- and belowground traits influence the  
455 magnitude of RPE. Along the duration of the experiment, the similar trend observed  
456 across all species of a peak of RPE after 120 days of plant growth suggests that the  
457 initial phase of plant growth was key in stimulating the RPE. This points out to a  
458 potential coupling between plant root phenology and the RPE. The following decrease  
459 observed across all species could be further interpreted as a lower impact of plants on  
460 the RPE once the pot has been fully colonized by roots. Growing root tips are indeed  
461 known to be very active in increasing root C inputs to soil (Paterson et al. 2006) and  
462 may therefore contribute disproportionately to RPE as the plant initially expands  
463 dramatically its root system to explore the surrounding soil volume. While  
464 environmental conditions could have played a role in these temporal patterns by

465 influencing plant relative growth rate, we did not observe an influence of relative  
466 growth rate on the RPE. Overall, it remains unclear whether that consistent trend of an  
467 early peak of RPE could represent an artefact of experimental manipulation or a realistic  
468 consequence of an actively growing root system and requires further testing.

469 Rhizosphere priming often has greater impact on the decomposition of soil C than  
470 the general priming effect induced by additions of substrates (e.g. glucose, plant  
471 residues) other than root exudates. Two meta-analyses have reported that on average,  
472 the general priming effect may speed the decomposition of SOC by *c.*14% (Luo et al.  
473 2015) or 27% (Zhang et al. 2013). By contrast, the average value of 82% RPE from our  
474 current study are 3-6 times higher than their values. In an experiment quantifying the  
475 priming effect of leaf litter additions from 15 tree species including some of the same  
476 species as studied here, Chao et al. (2019) also observed an average priming effect of  
477 11%, that is, a value 86% lower than the RPE recorded here. This difference may have  
478 several causes. First, the rhizosphere is the hot spot of root exudation, and the total  
479 amount of C entering the soil via root exudation is likely higher than C inputs from  
480 plant yearly litter productions in this study would be higher than this of litter input  
481 realistic studies of litter addition. In addition, root exudation of carbohydrates, which  
482 could be preferentially utilized by soil microbiota, may arguably be able to alleviate  
483 energy limitation in microbial activity more consistently along time and therefore to  
484 stimulate SOC decomposition (Finzi et al. 2015, Soong et al. 2020) more efficiently  
485 than discrete litter inputs to soils. Third, the presence of plants generally increases SOC  
486 decomposition due to the destruction of soil aggregates by living roots, as compared

487 the sole release of exudates (e.g. Bengtson et al. 2012), which leads to lower physical  
488 protection of soil organic matter and a greater release of mineral-protected C for  
489 microbial decomposition (He et al. 2020, Wang et al. 2020). Fourth, plant roots release  
490 oxalic acid and other organic acids, which have strong metal chelators abilities and can  
491 further disrupt mineral-organic associations (Keiluweit et al. 2015). Finally, the uptake  
492 of nutrients by roots could induce microbial growth to be limited by nutrients (rather  
493 than C or energy provided by rhizodeposition), thereby leading microbes to decompose  
494 nutrient-rich SOM to acquire nutrients: the mining hypothesis (Craine et al. 2007).  
495 Overall, the consistently high RPE observed here across eight contrasting species of  
496 trees and the much higher effect as compared to soil priming effects due to litter input  
497 suggest that several of these processes are likely to happen concomitantly to determine  
498 the major role of the RPE in global C cycling processes.

499

### 500 **Root traits control rhizosphere priming**

501 Our results only poorly support our first hypothesis that the RPE positively  
502 covaries with high biomass, fine root length, root branching density and root exudation  
503 rate. Taken individually, only high root exudate-derived respiration, considered as  
504 representative for root exudation rate, induced a marginally higher RPE. Since the role  
505 of root exudates in driving the RPE is well documented (e.g. Wang et al. 2016,  
506 Henneron et al. 2019), this result suggests that our estimate of CO<sub>2</sub> released during an  
507 incubation of rhizospheric soil may not have accurately reflected the effects of root  
508 exudates on the RPE (but see Henneron et al. 2019). One reason for this is that our

509 rhizospheric soil, sampled at the end of the experiment, had already experienced  
510 substantial priming during the 204 days of plant growth and may not well represent  
511 what has happened during the experimental period. Second, the rhizospheric soil is  
512 incubated in Mason jar where no live root exudation is taking place, as compared to the  
513 pots with live plants. Therefore, the root exudate-derived respiration appears unable to  
514 capture the short-term effect of root exudation.

515       Whereas most of our hypothesized root trait effects were non-significant, we  
516 observed a negative relationship between the RPE and root branching density. We  
517 expected that higher root branching density would be mainly representative of higher  
518 root tip numbers and therefore higher potential exudation capacities, but lower  
519 branching density might also enable larger soil volume exploration and thus be most  
520 effective for enhancing root effects on a larger soil volume (Freschet et al. 2021b).  
521 Additionally, a high root branching density contributes to greater enmeshment of soil  
522 particles and increases soil aggregate stability, which may play a non-negligible role in  
523 limiting SOC mineralization rates (Poirier et al. 2018).

524       In support for our second hypothesis, the three root traits that influenced the RPE  
525 to some extent (i.e. mean diameter of first-order roots, root branching density and root  
526 exudate-derived respiration) represented three complementary aspects of root structure  
527 and function (morphology, architecture and physiology, respectively). Mean diameter  
528 of first-order roots represents the type of economics strategy of the root (e.g. the reliance  
529 on mycorrhizal association; Bergmann et al., 2020), whereas root branching density is  
530 a key driver of the strategy of root to explore versus exploit the soil volume, and root

531 exudate-derived respiration relates to the activity of the roots per unit mass of root  
532 deployed. However, surprisingly, we found no relationship between any measure of  
533 plant biomass (e.g. specific organ biomass, total biomass) and the RPE. This is in  
534 contrast to a recent meta-analysis showing that plant total and aboveground biomass  
535 were correlated with the RPE (Huo et al. 2017). Indeed, plants that have higher biomass  
536 may generally allocate more labile C into soil surrounding the root and thereby intensify  
537 the mineralization of native soil C (Dijkstra et al. 2006). Nonetheless, different species  
538 differ in a broad range of root traits (Sun et al. 2021, Freschet et al. 2021a) and in their  
539 nutrient use efficiency (Henneron et al. 2020), so that estimates of plant biomass may  
540 not always reflect well plant nutrient requirements and acquisition, and consequently  
541 their influence on soil C priming. Moreover, plant biomass and growth rate were  
542 relatively similar in this study, reducing therefore the potential for these parameters to  
543 influence the RPE.

544       Among our eight tree species, the strongest predictor of the RPE was the mean  
545 diameter of first-order roots, possibly due to its central position in the network of root  
546 trait relationships. Particularly, higher mean diameter of first-order roots negatively  
547 influences root branching density (Eissenstat et al. 2015), as also observed here, and  
548 this has positive consequences for the RPE, as revealed by our path analysis. Among  
549 our tree species, higher mean diameter of first-order roots also positively influences  
550 root exudate-derived respiration, indicating a potentially higher production of exudates,  
551 also with positive consequences on the RPE. This positive relationship may have  
552 several causes. First, higher mean diameter of first-order roots implies higher

553 proportion of cortex tissues in the root, and therefore higher metabolic activity of the  
554 root with potential link to exudation processes (Ding et al., 2019; Freschet et al., 2021b;  
555 Kong et al., 2019). Second, higher mean diameter of first-order roots may imply higher  
556 reliance of thicker roots on mycorrhizal colonization (Kong et al., 2014; Paterson et al.  
557 2016, Bergmann et al. 2020), increased transfer of carbon to the fungal symbiont and  
558 increased mycorrhizal fungi exudation. Part of the increased root exudate-derived  
559 respiration observed in thicker roots may indeed be attributed to the action of  
560 mycorrhizal fungi fed by plant carbon allocation as mycorrhizal fungi have an important  
561 role in enzyme exudation and soil carbon priming (Bradford 2014, Yin et al. 2020).  
562 Mycorrhizal associations are indeed an efficient way to increase the volume of soil  
563 under influence of the root system and have particular abilities to degrade SOC (Frey  
564 2019, Yin et al. 2021), which will require further attention in future studies exploring  
565 the drivers of root effect on the RPE.

566

## 567 **Conclusion**

568 We demonstrated here that several aspects of root structure and function (i.e. mean  
569 diameter of first-order roots, root branching density and root exudate-derived  
570 respiration) have complementary influences on the magnitude of the RPE. This work  
571 illustrates how measuring comprehensive sets of plant traits, including aspects of plant  
572 root morphology, architecture and physiology, is necessary to adequately capture the  
573 effects of plants on soil functioning. However, future assessment will need to further  
574 include one potentially important aspect of root effect on the RPE, that is, plant reliance

575 on mycorrhizal colonization and mycorrhizal traits. Nonetheless, we identified a central  
576 role for the mean diameter of first-order roots, potentially via its influence on several  
577 other traits with likely more direct link to soil carbon priming. As first-order root  
578 diameter can be routinely measured, the role of this trait in plant RPE could offer a  
579 rough but useful first estimation of the RPE, if confirmed over wider range of species  
580 and environmental conditions.

581 Overall, our results confirm the potential use of root traits to predict the integrated  
582 response of soil C dynamics to changes in species composition under future climate  
583 change (Cheng et al. 2014, Finzi et al. 2015, Henneron et al. 2020). Although our use  
584 of a non-native soil (the C<sub>4</sub> soil) and small tree seedlings planted in pots likely  
585 misrepresent the influence of mature trees grown in field ecosystems (Mokany and Ash  
586 2008, Freschet et al. 2017, Yin et al. 2018), they yield promising results that should  
587 open the way to further experiments with larger number of species and more realistic  
588 field conditions.

589 *Acknowledgements* – We thank Xin Yu for help with the experiment.

590 *Funding* – This research was funded by the National Key Research and Development  
591 Program of China (2022YFF1303003 and 2021YFD2201303), key Project of Jiangxi  
592 Province Natural Science Foundation of China (20224ACB205003), National Natural  
593 Science Foundation of China (U22A20612, 32201540 and 42177289) and the Natural  
594 Science Foundation of Guangxi (2021GXNSFBA196021). Lin Chao was further  
595 supported by the Youth Talent Exchange and Cooperation Foundation of the Key  
596 Laboratory of Forest Ecology and Management of the Chinese Academy of Sciences to

597 work at the CEFE in Montpellier (France). GTF was supported by the "Laboratoires  
598 d'Excellences (LABEX)" TULIP (ANR-10-LABX-41).

## 599 **References**

- 600 Ataka, M., Sun, L. J., Nakaji, T., Katayama, A. and Hiura, T. 2020. Five-year nitrogen  
601 addition affects fine root exudation and its correlation with root respiration in a  
602 dominant species, *Quercus crispula*, of a cool temperate forest, Japan. *Tree Physiol.*  
603 40: 367–376.
- 604 Bais, H. P., Weir T. L., T., Perry, L. G., Gilroy, S. and Vivanco, J. M. 2006. The role of  
605 root exudates in rhizosphere interactions with plants and other organisms. *Annu*  
606 *Rev Plant Biol.* 57: 233–266.
- 607 Bardgett, R. D., Mommer, L. and De Vries, F.T. 2014. Going underground: root traits  
608 as drivers of ecosystem processes. *Trends Ecol. Evol.* 29: 692–699.
- 609 Bengtson, P., Barker, J. and Grayston, S. J. 2012. Evidence of a strong coupling between  
610 root exudation, C and N availability, and stimulated SOM decomposition caused  
611 by rhizosphere priming effects. *Ecol Evol.* 2: 1843–1852.
- 612 Bergmann, J., Weigelt, A., van der Plas, F., Laughlin, D. C., Kuyper, T. W., Guerrero-  
613 Ramirez, N., Valverde-Barrantes, O. J., Bruelheide, H., Freschet, G. T., Iversen, C.  
614 M., Kattge, J., McCormack, M. L., Meier, I. C., Rillig, M. C., Roumet, C.,  
615 Semchenko, M., Sweeney, C. J., van Ruijven, York, L. M. and Mommer, L. 2020.  
616 The fungal collaboration gradient dominates the root economics space in plants.  
617 *Sci Adv.* 6: eaba3756.
- 618 Bradford, M. A. 2014. Good dirt with good friends. *Nature.* 505: 486–487.
- 619 Brzostek, E. R., Dragoni, D., Brown, Z. A. and Phillips, R. P. 2015. Mycorrhizal type  
620 determines the magnitude and direction of root-induced changes in decomposition  
621 in a temperate forest. *New Phytol.* 206: 1274–1282.

622 Canarini, Kaiser, C., Merchant, A., Richter, A. and Wanek, W., A. 2019. Root exudation  
623 of primary metabolites: mechanisms and their roles in plant responses to  
624 environmental stimuli. *Front Plant Sci.* 10: 157.

625 Carrillo, Y., Bell, C., Koyama, A., Canarini, A., Boot, C. M., Wallenstein, M. and  
626 Pendall, E. 2017. Plant traits, stoichiometry and microbes as drivers of  
627 decomposition in the rhizosphere in a temperate grassland. *J Ecol.* 105: 1750–1765.

628 Chang, Q., Qu, G. F., Xu, W. H., Wang, C., Cheng, W. X. and Bai, E. 2020. Light  
629 availability controls rhizosphere priming effect of temperate forest trees. *Soil Biol  
630 Biochem.* 14: 8107895

631 Chao, L., Liu, Y., Freschet, G. T., Zhang, W. D., Yu, X., Zheng, W. H., Guan, X., Yang,  
632 Q. P., Chen, L. C., Dijkstra, F. A. and Wang, S. L. 2019. Litter carbon and nutrient  
633 chemistry control the magnitude of soil priming effect. *Funct Ecol.* 33: 876–888.

634 Cheng, W. X. and Kuzyakov, Y. 2005. Root effects on soil organic matter decomposition.  
635 In: Zobel, R.W., Wright, S.F. (Eds.), *Roots and Soil Management: Interactions  
636 between Roots and the Soil*, Agronomy Monograph No. 48. American Society of  
637 Agronomy, Crop Science Society of America, Soil Science Society of America,  
638 Madison, WI, USA, pp. 119–143.

639 Cheng, W. X., Johnson, D. W. and Fu, S. L. 2003. Rhizosphere effects on decomposition:  
640 controls of plant species, phenology, and fertilization. *Soil Sci Soc Am J.* 67:  
641 1418–1427.

642 Cheng, W. X., Parton, W. J., Gonzalez-Meler, M. A., Phillips, R., Asao, S., McNickle,  
643 G. G., Brzostek, E. and Jastrow, J. D. 2014. Synthesis and modeling perspectives  
644 of rhizosphere priming. *New Phytol.* 201: 31–44.

645 Cotrufo, M. F., Soong, J. L., Horton, A. J., Campbell, E. E., Haddix, M. L., Wall, D. H.  
646 and Parton, W. J. 2015. Formation of soil organic matter via biochemical and

647 physical pathways of litter mass loss. *Nat Geosci.* 8: 776–779.

648 Craine, J. M., Morrow, C. and Fierer, N. 2007. Microbial nitrogen limitation increases  
649 decomposition. *Ecology.* 88: 2105–2113.

650 Davidson, E. A. and Janssens, I. A. 2006. Temperature sensitivity of soil carbon  
651 decomposition and feedbacks to climate change. *Nature.* 440: 165–173.

652 Dijkstra, F. A., Carrillo, Y., Pendall, E. and Morgan, J.A. 2013. Rhizosphere priming: a  
653 nutrient perspective. *Front Microbiol.* 4: 216.

654 Dijkstra, F. A., Cheng, W. X., and Johnson, D.W. 2006. Plant biomass influences  
655 rhizosphere priming effects on soil organic matter decomposition in two  
656 differently managed soils. *Soil Biol Biochem.* 38: 2519–2526.

657 Dijkstra, F. A., Morgan, J. A., Blumenthal, D. and Follett, R. F. 2010. Water limitation  
658 and plant inter-specific competition reduce rhizosphere-induced C decomposition  
659 and plant N uptake. *Soil Bio Biochem.* 42: 1073-1082.

660 Ding, J. X., Kong, D. L., Zhang, Z. L., Cai, Q., Xiao, J., Liu, Q. and Yin, H. J. et al.  
661 2020. Climate and soil nutrients differentially drive multidimensional fine root  
662 traits in ectomycorrhizal dominated alpine coniferous forests. *J Ecol.* 108: 2544–  
663 2556.

664 Eissenstat, D. M., Kucharski, J. M., Zadworny, M., Adams, T. S. and Koide, R.T. 2015.  
665 Linking root traits to nutrient foraging in arbuscular mycorrhizal trees in a  
666 temperate forest. *New Phytol.* 208: 114–124.

667 Finzi, A. C., Abramoff, R. Z., Spiller, K. S., Brzostek, E. R., Darby, B. A., Kramer, M.  
668 A. and Phillips, R.P. 2015. Rhizosphere processes are quantitatively important  
669 components of terrestrial carbon and nutrient cycles. *Glob Chang Biol.* 21: 2082–  
670 2094.

671 Fischer, H., Ingwersen, J. and Kuzyakov, Y. 2010. Microbial uptake of low-molecular

672 weight organic substances out-competes sorption in soil. *Eur J Soil Sci.* 61: 504–  
673 513.

674 Fontaine, S., Barot, S., Barré, P., Bdioui, N., Mary, B. and Rumpel, C. 2007. Stability  
675 of organic carbon in deep soil layers controlled by fresh carbon supply. *Nature.*  
676 450: 277–280.

677 Freschet, G. T., Pagès, L., Iversen, C. M., Comas, L. H., Rewald, B., Roumet, C.,  
678 Klimesova, J., Zadworny, M., Poorter, H., Postma, J. A., Adams, T. S.,  
679 Bagniewska-Zadworna, A., Bengough, A. G., Blancaflor, E. B., Brunner, I.,  
680 Cornelissen, J. H. C., Garnier, E., Gessler, A., Hobbie, S. E., Meier, I. C., Mommer,  
681 L., Picon-Cochard, C., Rose, L., Ryser, P., Scherer-Lorenzen, M., Soudzilovskaia,  
682 N. A., Stokes, A., Sun, T., Valverde-Barrantes, O. J., Weemstra, M., Weigelt, A.,  
683 Wurzbürger, N., York, L. M., Batterman, S. A., Gomes de Moraes, M., Janecek, S.,  
684 Lambers, H., Salmon, V., Tharayil, N. and McCormack, M. L. 2021b. A starting  
685 guide to root ecology: strengthening ecological concepts and standardizing root  
686 classification, sampling, processing and trait measurements. *New Phytol.* 232:  
687 973–1122.

688 Freschet, G. T., Roumet, C., Comas, L. H., Weemstra, M., Bengough, A. G., Rewald,  
689 B., Bardgett, R. D., De Deyn, G. B., Johnson, D., Klimešová, J., Lukac, M.,  
690 McCormack, M. K., Meier, I.C., Pagès, L., Poorter, H., Prieto, I., Wurzbürger, N.,  
691 Zadworny, M., Bagniewska-Zadworna, A., Blancaflor, E. B., Brunner, I., Gessler,  
692 A., Hobbie, S. E., Iversen, C.M., Mommer, L., Picon-Cochard, C., Postma, J. A.,  
693 Rose, L., Ryser, P., Scherer-Lorenzen, M., Soudzilovskaia, N.A., Sun, T.,  
694 Valverde-Barrantes, O. J., Weigelt, A, York, L. M., Stokes, A. 2021a. Root traits  
695 as drivers of plant and ecosystem functioning: current understanding, pitfalls and  
696 future research needs. *New Phytol.* 232: 1123–1158.

697 Freschet, G. T., Valverde-Barrantes, O. J., Tucker, C. M., Craine, J. M., McCormack, M.  
698 L., Violle, C., Fort, F., Blackwood, C. B., Urban-Mead, K. R., Iversen, C. M.,  
699 Bonis, A., Comas, L. H., Cornelissen, J. H. C., Dong, M., Guo, D. L., Hobbie, S.  
700 E., Holdaway, R. J., Kembel, S. W., Makita, N., Onipchenko, V.G., Picon-Cochard,  
701 C., Reich, P. B., de la Riva, E. G., Smith, S. W., Soudzilovskaia, N. A., Tjoelker,  
702 M. G., Wardle, D. A. and Roumet, C. 2017. Climate, soil and plant functional types  
703 as drivers of global fine-root trait variation. *J Ecol.* 105: 1182–1196.

704 Freschet, G.T. and Roumet, C., 2017. Sampling roots to capture plant and soil functions.  
705 *Functional Ecology* 31, 1506–1518.

706 Frey, S. D. 2019. Mycorrhizal fungi as mediators of soil organic matter dynamics. *Annu*  
707 *Rev Ecol Evol S.* 50: 237–259.

708 Girkin, N.T., Turner, B. L., Ostle, N. and Sjögersten, S. 2018. Composition and  
709 concentration of root exudate analogues regulate greenhouse gas fluxes from  
710 tropical peat. *Soil Biol. Biochem.* 127, 280–285

711 Gougherty, S. W., Bauer, J. E. and Pohlman, J. W. 2018. Exudation rates and  $\delta^{13}\text{C}$   
712 signatures of tree root soluble organic carbon in a riparian forest. *Biochemistry.*  
713 137: 235-252

714 Guenet, B., Camino-Serrano, M., Ciais, P., Tifafi, M., Maignan, F., Soong, J. L. and  
715 Janssens, I. A. 2018. Impact of priming on global soil carbon stocks. *Glob Chang*  
716 *Biol.* 24: 1873–1883.

717 Han, M. G., Sun L. J., Gan, D. Y., Fu, L. C. and Zhu, B. 2020. Root functional traits are  
718 key determinants of the rhizosphere effect on soil organic matter decomposition  
719 across 14 temperate hardwood species. *Soil Biol Biochem.* 151: 108019

720 He, Y. H., Cheng, W. X., Zhou, L.Y., Shao, J.J., Liu, H.Y., Zhou, H.M., Zhu, K. and  
721 Zhou, X. H. 2020. Soil DOC release and aggregate disruption mediate rhizosphere

722 priming effect on soil C decomposition. *Soil Biol Biochem.* 144: 107787.

723 Heimann, M. and Reichstein, M. 2008. Terrestrial ecosystem carbon dynamics and  
724 climate feedbacks. *Nature.* 451: 289–292.

725 Henneron, L., Cros, C., Picon-Cochard, C., Rahimian, V., Fontaine, S. and Vries, F.  
726 2019. Plant economic strategies of grassland species control soil carbon dynamics  
727 through rhizodeposition. *J Ecol.* 108: 528–545.

728 Henneron, L., Kardol P, Wardle D. A, Cros C and Fontaine S. 2020. Rhizosphere control  
729 of soil nitrogen cycling: a key component of plant economic strategies. *New*  
730 *Phytol.* 228: 1269–1282.

731 Huo, C., Luo, Y. Q. and Cheng, W. X. 2017. Rhizosphere priming effect: a meta-  
732 analysis. *Soil Biol Biochem.* 111: 78–84.

733 Keiluweit, M., Bougoure, J. J., Nico, P. S., Pett-Ridge, J., Weber, P. K. and Kleber, M.  
734 2015. Mineral protection of soil carbon counteracted by root exudates. *Nat Clim*  
735 *Chang.* 5: 588–595.

736 Kong, D. L., Wang J. J, Wu, H. F., Valverde-Barrantes, O. J., Wang, R., Zeng, H., Kardol,  
737 P., Zhang, H. Y. and Feng Y. L. 2019. Nonlinearity of root trait relationships and  
738 the root economics spectrum. *Nat Commun.* 10: 2203.

739 Kong, D., Ma, C., Zhang, Q., Li, L., Chen, X., Zeng, H. and Guo, D. 2014. Leading  
740 dimensions in absorptive root trait variation across 96 subtropical forest species.  
741 *New Phytol* 203: 863–872.

742 Kumar. A., Phillips, R. P., Scheibe, A., Klink, S. and Pausch, J. 2020. Organic matter  
743 priming by invasive plants depends on dominant mycorrhizal association. *Soil*  
744 *Biol Biochem.* 140: 107645.

745 Kuzyakov, Y. 2002. Review: factors affecting rhizosphere priming effects. *J Plant Nutr*  
746 *Soil Sc.* 165: 382–396.

747 Kuzyakov, Y. and Cheng, W. X. 2001. Photosynthesis controls of rhizosphere  
748 respiration and organic matter decomposition. *Soil Biol Biochem.* 33: 1915–1925.

749 Kuzyakov, Y. and Cheng, W. X. 2004. Photosynthesis controls of CO<sub>2</sub> efflux from  
750 maize rhizosphere. *Plant Soil.* 263: 85–99.

751 Kuzyakov, Y. and Xu, X. L. 2013. Competition between roots and microorganisms for  
752 nitrogen: mechanisms and ecological relevance. *New Phytol.* 198: 656-669.

753 Li, J., Zhou, M. Y., Alaei, S. and Bengtson, P. 2020. Rhizosphere priming effects differ  
754 between Norway spruce (*Picea abies*) and Scots pine seedlings cultivated under  
755 two levels of light intensity. *Soil Biol Biochem.* 145: 107788.

756 McCormack, M. L., Dickie, I. A., Eissenstat, D. M., Fahey, T. J., Fernandez, C. W., Guo,  
757 D., Helmisaari, H. S., Hobbie, E. A., Iversen, C. M., Jackson, R. B., Leppalammi-  
758 Kujansuu, J., Norby, R. J., Phillips, R. P., Pregitzer, K. S., Pritchard, S. G., Rewald,  
759 B. and Zadworny, M. 2015. Redefining fine roots improves understanding of  
760 below-ground contributions to terrestrial biosphere processes. *New Phytol.* 207:  
761 505–518.

762 Meier, I. C., Tückmantel, T., Heitkötter, J., Muller, K., Preusser, S., Wrobel, T. J.,  
763 Kandeler, E., Marschner, B. and Leuschner, C. 2020. Root exudation of mature  
764 beech forests across a nutrient availability gradient: the role of root morphology  
765 and fungal activity. *New Phytol.* 226: 583–594.

766 Mokany, K. and Ash, J. 2008. Are traits measured on pot grown plants representative  
767 of those in natural communities? *J Veg Sci.* 19: 119–126.

768 Paterson, E. et al. 2016. Arbuscular mycorrhizal hyphae promote priming of native soil  
769 organic matter mineralisation. *Plant Soil.* 408: 243–254.

770 Paterson, E., Sim, A., Davidson, J. and Daniell, T. J. 2006. Root exudation from  
771 *Hordeum vulgare* in response to localized nitrate supply. *J. Exp. Bot.* 57: 2413–

772           2420.

773 Pausch, J., Zhu, B., Kuzyakov, Y. and Cheng, W. X. 2013. Plant inter-species effects on  
774           rhizosphere priming of soil organic matter decomposition. *Soil Biology Biochem.*  
775           57: 91–99.

776 Phillips, R. P. and Fahey, T. J. 2006. Tree species and mycorrhizal associations influence  
777           the magnitude of rhizosphere effects. *Ecology.* 87: 1302–1313.

778 Poirier, V., Roumet, C. and Munson, A. D. 2018. The root of the matter: linking root  
779           traits and soil organic matter stabilization processes. *Soil Biology Biochem.* 120:  
780           246–259.

781 Pregitzer, K. S., DeForest, J. L., Burton, A. J., Allen, M. F., Ruess, R. W. and Hendrick,  
782           R. L. 2002. Fine root architecture of nine North American trees. *Ecol Monogr.*  
783           72: 293–309.

784 Qiao, N., Schaefer, D., Blagodatskaya, E., Zou, X., Xu, X. and Kuzyakov, Y. 2013.  
785           Labile carbon retention compensates for CO<sub>2</sub> released by priming in forest soils.  
786           *Global Change Biol.* 20: 1943–1954.

787 Rosseel, Y. 2012. lavaan: an R package for structural equation modeling. *J Stat Softw.*  
788           48: 1–36.

789 Schmidt, M. W. I., Torn, M. S., Abiven, S., Dittmar, T., Guggenberger, G., Janssens, I.  
790           A. and Trumbore, S. E. 2011. Persistence of soil organic matter as an ecosystem  
791           property. *Nature.* 478: 49–56.

792 Schnyder, H. and Lattanzi, F. A. 2005. Partitioning respiration of C<sub>3</sub>–C<sub>4</sub> mixed  
793           communities using the natural abundance <sup>13</sup>C approach – testing assumptions in a  
794           controlled environment. *Plant Biol.* 7: 592–600.

795 Shahzad, T., Chenu, C., Genet, P., Barot, S., Perveen, N., Mougin, C. and Fontaine, S.  
796           2015. Contribution of exudates, arbuscular mycorrhizal fungi and litter depositions

797 to the rhizosphere priming effect induced by grassland species. *Soil Biology*  
798 *Biochem.* 80: 146–155.

799 Shipley, B. 2015. *Cause and Correlation in Biology: A User's Guide to Path Analysis,*  
800 *Structural Equations and Causal Inference.* Cambridge University press,  
801 Cambridge, UK.

802 Soong, J. L., Fuchslueger, L., Marañon-Jimenez, S., Torn, M. S., Janssens, I. A.,  
803 Penuelas, J. and Richter, A. 2020. Microbial carbon limitation: The need for  
804 integrating microorganisms into our understanding of ecosystem carbon cycling.  
805 *Global Change Biol.* 26: 1953–1961.

806 Sun, L., Ataka, M., Han, M., Han, Y., Gan, D., Xu, T., Guo, Y., and Zhu, B. 2021. Root  
807 exudation as a major competitive fine-root functional trait of 18 coexisting species  
808 in a subtropical forest. *New Phytol.* 229: 259–271.

809 Tang, M., Cheng, W. X., Zeng, H. and Zhu, B. 2019. Light intensity controls  
810 rhizosphere respiration rate and rhizosphere priming effect of soybean and  
811 sunflower. *Rhizosphere.* 9: 97–105.

812 Thurgood, A., Singh, B., Jones, E. and Barbour, M. M. 2014. Temperature sensitivity  
813 of soil and root respiration in contrasting soils. *Plant Soil.* 382: 253–267.

814 Tifafi, M., Guenet, B. and Hatté, C. 2018. Large Differences in Global and Regional  
815 Total Soil Carbon Stock Estimates Based on Soil Grids, HWSD, and NCSCD:  
816 Intercomparison and Evaluation Based on Field Data From USA, England, Wales,  
817 and France. *Global Biogeochem Cy.* 32: 42–56.

818 Wang, X. H., Yin, L. M., Dijkstra, F. A., Lu, J.Y., Wang, P. and Cheng, W. X. 2020.  
819 Rhizosphere priming is tightly associated with root-driven aggregate turnover. *Soil*  
820 *Biol Biochem.* 149: 107964.

821 Wang, X. J., Tang, C. X., Severi, J., Butterly, C. R. and Baldock, J. A. 2016. Rhizosphere

822 priming effect on soil organic carbon decomposition under p-lant species differing  
823 in soil acidification and root exudation. *New Phytol.* 211: 864–873.

824 Wen, Z., Shen, Q., Tang, X., Xiong, C., Li, H., Pang, J., Ryan, M. H., Lambers, H. and  
825 Shen, J. 2019. Tradeoffs among root morphology, exudation and mycorrhizal  
826 symbioses for phosphorus-acquisition strategies of 16 crop species. *New Phytol.*  
827 223: 882–895.

828 Yin, L. M., Dijkstra, F. A., Phillips, R. P., Zhu, B., Wang, P. and Cheng, W. X. 2021.  
829 Arbuscular mycorrhizal trees cause a higher carbon to nitrogen ratio of soil organic  
830 matter decomposition via rhizosphere priming than ectomycorrhizal trees. *Soil*  
831 *Biol Biochem.* 157: 108246.

832 Yin, L. M., Xiao, W., Dijkstra, F. A., Zhu, B., Wang, P. and Cheng, W. X. 2020. Linking  
833 absorptive roots and their functional traits with rhizosphere priming of tree species.  
834 *Soil Biol Biochem.* 150: 107997.

835 Yin, L., Dijkstra, F. A., Wang, P., Zhu, B. and Cheng, W. 2018. Rhizosphere priming  
836 effects on soil carbon and nitrogen dynamics among tree species with and without  
837 intraspecific competition. *New Phytol.* 218: 1036–1048.

838 Zhu, B. and Cheng, W. 2011. Rhizosphere priming effect increases the temperature  
839 sensitivity of soil organic matter decomposition. *Global Change Biol.* 17: 2172–  
840 2183.

841 Zhu, B. and Cheng, W. 2013. Impacts of drying–wetting cycles on rhizosphere  
842 respiration and soil organic matter decomposition. *Soil Biol Biochem.* 63: 89–96.

843 Zhu, B., Gutknecht, J. L. M., Herman, D. J., Keck, D. C., Firestone, M. K. and Cheng,  
844 W. X. 2014. Rhizosphere priming effects on soil carbon and nitrogen  
845 mineralization. *Soil Biol Biochem.* 76: 183–192.

846

847

848 **Figure Captions:**

849 **Figure 1** Change in CO<sub>2</sub> efflux from microcosms induced by eight plant species along  
850 204 days of growth. CO<sub>2</sub> efflux from an unplanted control (black lines with squares),  
851 as well as the total CO<sub>2</sub> (red lines with circles), soil-derived CO<sub>2</sub> (blue lines with  
852 triangles), plant-derived CO<sub>2</sub> (pink lines with inverted triangles) and priming of SOC  
853 (green lines with diamonds) induced by plants are represented for each species. Values  
854 are mean  $\pm$  SE.

855 **Figure 2** Mean daily (a) soil organic matter (SOM-)derived CO<sub>2</sub>, plant-derived CO<sub>2</sub>  
856 and CO<sub>2</sub> associated to the primed C (data above the bars), (b) rhizosphere priming effect,  
857 and (c) root exudate-derived CO<sub>2</sub> along the 204 days of growth in planted treatments.  
858 Sub-legend shows ANOVA *P* values. Values are mean  $\pm$  SE; *n*=5 for all treatments  
859 except for *n*=4 for *Quercus acutissima*, *Carya cathayensis* and *Schima superba*  
860 treatments.

861 **Figure 3** Relationships between the rhizosphere priming effect and (a) mean first-order  
862 root diameter, (b) root branching density, and (c) root exudate-derived respiration. The  
863 means of each species are plotted and error bars represent  $\pm$  SE; *n*=5 for all treatments  
864 except for *n*=4 for *Quercus acutissima*, *Carya cathayensis* and *Schima superba*  
865 treatments. Strength (*R*<sup>2</sup>) and significance (*P*) of linear regressions are displayed when  
866 (marginally-) significant. The filled areas indicate the 95% confidence interval.

867 **Figure 4** (a) Initial and (b) final path models of the influence of plant belowground  
868 traits on the rhizosphere priming effect (RPE). The initial path model shows a  
869 significant misfit, whereas the final most probable path model shows no significant

870 misfit between the empirical data and the causal structure specified by the models.  
871 Boxes are measured variables and arrows represent hypothesized causal links.  
872 Regarding the final path model (**b.**), values on the lines are the standardized path  
873 coefficients between the causal variable and the caused variable. All path coefficients  
874 are significantly different from zero (solid lines), or marginally significant where  $P$ -  
875 values are displayed next to path coefficients (dashed lines). The  $R^2$  represent the  
876 percentage of variance explained by the causal variables. Green and orange lines  
877 indicate positive and negative relationships, respectively. Thickness of the lines is  
878 proportional to the strength of path coefficients. For all traits, we used the average value  
879 of five individuals per species.  $R_{\text{exudates}}$  is root exudate-derived respiration;  $\text{SRL}_{1\text{st}}$  is  
880 specific root length of the first-order roots;  $\text{MRD}_{1\text{st}}$  is mean root diameter of the first-  
881 order roots; RBD is root branching density;  $\text{RB}_{1\text{st}}$  is biomass of the first-order roots;  
882  $\text{RTD}_{1\text{st}}$  is root tissue density of the first-order roots;  $\text{RL}_{1\text{st}}$  is root length of the first-order  
883 roots.

884 **Table 1** Plant biomass and root functional traits at the end of the experiment. Values  
885 represent means  $\pm$  SE;  $n=5$  for all treatments, except for *Quercus acutissima*, *Carya*  
886 *cathayensis* and *Schima superba* treatments where  $n=4$ . Different letters indicate  
887 significant differences among species (post hoc Tukey–Kramer honest significant  
888 difference (HSD) test,  $P < 0.05$ ). ECM, ectomycorrhizal; AM, arbuscular.  
889

Species	<i>Liquidambar formosana</i>	<i>Quercus acutissima</i>	<i>Carya cathayensis</i>	<i>Cunninghamia lanceolata</i>	<i>Ginkgo biloba</i>	<i>Schima superba</i>	<i>Triadica sebifera</i>	<i>Zanthoxylum bungeanum</i>	CV (%)
Family	Altingiaceae	Fagaceae	Juglandaceae	Cupressaceae	Ginkgoaceae	Theaceae	Euphorbiaceae	Rutaceae	
Growth form	Deciduous broadleaf	Deciduous broadleaf	Deciduous broadleaf	Evergreen broadleaf	Deciduous broadleaf	Deciduous broadleaf	Deciduous broadleaf	Deciduous broadleaf	
Mycorrhizal types	ECM	ECM	ECM	AM	AM	AM	AM	AM	
<i>Plant biomass</i>									
Plant total biomass (g per pot)	4.3 $\pm$ 1.0a	9.6 $\pm$ 1.3b	12.0 $\pm$ 1.7bc	15.0 $\pm$ 1.9c	7.2 $\pm$ 0.4ab	3.8 $\pm$ 0.3a	11.1 $\pm$ 0.7bc	7.1 $\pm$ 0.4ab	40.9
Aboveground biomass (g per pot)	2.8 $\pm$ 0.6a	5.0 $\pm$ 1.0ab	7.8 $\pm$ 0.9c	8.2 $\pm$ 0.7c	4.1 $\pm$ 0.3a	2.6 $\pm$ 0.3a	6.8 $\pm$ 0.4bc	4.0 $\pm$ 0.2a	40.0
Belowground biomass (g per pot)	1.5 $\pm$ 0.4ab	4.5 $\pm$ 0.6cd	4.2 $\pm$ 0.8bcd	6.7 $\pm$ 1.2d	3.2 $\pm$ 0.2abc	1.2 $\pm$ 0.1a	4.3 $\pm$ 0.5bcd	3.1 $\pm$ 0.2abc	44.1
Leaf biomass (g per pot)	0.2 $\pm$ 0.1ab	0.4 $\pm$ 0.1cd	1.5 $\pm$ 0.4bc	4.0 $\pm$ 0.4d	1.1 $\pm$ 0.1abc	0.5 $\pm$ 0.1a	2.6 $\pm$ 0.1bcd	1.2 $\pm$ 0.1abc	78.6
First-order root biomass (g per pot)	0.01 $\pm$ 0.0a	0.02 $\pm$ 0.0a	0.01 $\pm$ 0.0a	0.28 $\pm$ 0.1bc	0.10 $\pm$ 0.0ab	0.01 $\pm$ 0.0a	0.39 $\pm$ 0.1c	0.44 $\pm$ 0.1c	100.6
Absorptive root biomass (g per pot)	0.06 $\pm$ 0.0a	0.21 $\pm$ 0.0ab	0.09 $\pm$ 0.0a	1.67 $\pm$ 0.4c	0.89 $\pm$ 0.1abc	1.02 $\pm$ 0.3bc	1.60 $\pm$ 0.1c	1.66 $\pm$ 0.2c	63.7
<i>Morphological root traits</i>									
Mean first-order root diameter (mm)	0.37 $\pm$ 0.0ab	0.50 $\pm$ 0.1cd	0.35 $\pm$ 0.1a	0.58 $\pm$ 0.0d	0.76 $\pm$ 0.0e	0.41 $\pm$ 0.0abc	0.33 $\pm$ 0.0a	0.49 $\pm$ 0.0bcd	27.0
Mean absorptive root diameter (mm)	0.64 $\pm$ 0.08ab	0.90 $\pm$ 0.08b	0.57 $\pm$ 0.07ab	0.88 $\pm$ 0.08b	1.24 $\pm$ 0.07c	1.63 $\pm$ 0.14d	0.42 $\pm$ 0.01a	0.73 $\pm$ 0.01ab	41.4
First-order root tissue density (g cm <sup>-3</sup> )	0.08 $\pm$ 0.01a	0.22 $\pm$ 0.06bc	0.06 $\pm$ 0.01a	0.13 $\pm$ 0.01ab	0.07 $\pm$ 0.00a	0.24 $\pm$ 0.04c	0.10 $\pm$ 0.01a	0.08 $\pm$ 0.01a	51.5
Absorptive root tissue density (g cm <sup>-3</sup> )	0.14 $\pm$ 0.03a	0.28 $\pm$ 0.02c	0.12 $\pm$ 0.02a	0.23 $\pm$ 0.02bc	0.16 $\pm$ 0.01ab	0.37 $\pm$ 0.02d	0.14 $\pm$ 0.01a	0.16 $\pm$ 0.02ab	40.1
First-order specific root length (m g <sup>-1</sup> )	116.2 $\pm$ 11.5c	33.4 $\pm$ 5.4ab	211.2 $\pm$ 21.0d	29.6 $\pm$ 1.8a	30.0 $\pm$ 0.7ab	37.0 $\pm$ 11.3a	118.8 $\pm$ 6.5c	77.7 $\pm$ 12.4bc	66.6
Absorptive specific root length (m g <sup>-1</sup> )	55.55 $\pm$ 15.1bc	7.99 $\pm$ 1.5a	69.12 $\pm$ 14.1c	10.92 $\pm$ 1.0a	8.34 $\pm$ 0.6a	1.49 $\pm$ 0.6a	64.64 $\pm$ 5.1bc	33.45 $\pm$ 2.9ab	81.8
<i>Architectural root traits</i>									
Root branching density (cm <sup>-1</sup> )	3.25 $\pm$ 0.54	2.65 $\pm$ 0.70	3.32 $\pm$ 0.70	1.76 $\pm$ 0.21	2.47 $\pm$ 0.33	3.85 $\pm$ 1.03	2.97 $\pm$ 0.32	1.97 $\pm$ 0.15	23.8
<i>Physiological root traits</i>									
Root exudate-derived respiration (mg C kg <sup>-1</sup> soil d <sup>-1</sup> )	0.42 $\pm$ 0.10ab	0.59 $\pm$ 0.09b	0.37 $\pm$ 0.02ab	0.49 $\pm$ 0.05ab	0.49 $\pm$ 0.03ab	0.34 $\pm$ 0.02ab	0.30 $\pm$ 0.06a	0.34 $\pm$ 0.04ab	21.9
Rhizosphere soil respiration (mg C kg <sup>-1</sup> soil d <sup>-1</sup> )	2.30 $\pm$ 0.08	2.16 $\pm$ 0.13	2.46 $\pm$ 0.11	2.36 $\pm$ 0.13	2.28 $\pm$ 0.12	2.08 $\pm$ 0.08	2.05 $\pm$ 0.04	2.34 $\pm$ 0.09	5.9
<i>Composite (biomass-related) root traits</i>									
First-order root length (m)	1.12 $\pm$ 0.2a	0.48 $\pm$ 0.1a	2.41 $\pm$ 0.5a	8.04 $\pm$ 2.1a	3.00 $\pm$ 0.5a	0.54 $\pm$ 0.2a	45.87 $\pm$ 5.7c	31.39 $\pm$ 2.2b	137.2
Absorptive root length (m)	2.04 $\pm$ 0.39ab	1.04 $\pm$ 0.20a	4.83 $\pm$ 0.92bc	15.11 $\pm$ 3.69d	5.86 $\pm$ 0.78c	0.90 $\pm$ 0.23a	87.66 $\pm$ 7.20e	50.10 $\pm$ 2.71e	138.9
First-order root length density (cm cm <sup>-3</sup> )	0.01 $\pm$ 0.003a	0.01 $\pm$ 0.001a	0.03 $\pm$ 0.006a	0.10 $\pm$ 0.026a	0.04 $\pm$ 0.006a	0.01 $\pm$ 0.002a	0.57 $\pm$ 0.070c	0.39 $\pm$ 0.027b	137.1
Absorptive root length density (cm cm <sup>-3</sup> )	0.01 $\pm$ 0.002a	0.01 $\pm$ 0.002a	0.03 $\pm$ 0.007a	0.08 $\pm$ 0.020a	0.03 $\pm$ 0.004a	0.00 $\pm$ 0.000a	0.50 $\pm$ 0.072c	0.23 $\pm$ 0.016b	143.0

890 **Table 2** Regression coefficient ( $\beta$ ), strength ( $R^2$ ) and significance ( $P$ ) of univariate  
891 linear regressions between descriptors of plant biomass and traits and the rhizosphere  
892 priming effect. (+/-) represents the sign of the relationship. Variables explaining the  
893 highest variation in RPE ( $R^2 > 0.4$ ) and subsequently retained for multivariate  
894 regression analyses are highlighted in bold.

	$\beta$ -value	$R^2$ (+/-)	$P$ -value
<i>Plant biomass</i>			
Plant total biomass	0.006	0.062 (+)	0.553
Aboveground biomass	0.006	0.022 (+)	0.726
Belowground biomass	0.020	0.135 (+)	0.370
Leaf biomass	0.023	0.091 (+)	0.467
First-order root biomass	-0.010	0.000 (-)	0.965
Absorptive root biomass	0.003	0.000 (+)	0.968
<i>Morphological root traits</i>			
<b>Mean first-order root diameter</b>	0.533	<b>0.607 (+)</b>	<b>0.023</b>
Mean absorptive root diameter	0.036	0.022 (+)	0.726
First-order root tissue density	-0.071	0.027 (-)	0.699
Absorptive root tissue density	0.005	0.000 (+)	0.984
First-order specific root length	-0.001	0.213 (-)	0.250
Absorptive specific root length	-0.002	0.190 (-)	0.281
<i>Architectural root traits</i>			
<b>Root branching density</b>	-0.096	<b>0.521 (-)</b>	<b>0.043</b>
<i>Physiological root traits</i>			
<b>Root exudate-derived respiration</b>	0.623	<b>0.424 (+)</b>	<b>0.080</b>
Rhizosphere soil respiration	0.375	0.317 (+)	0.146
Plant-derived CO <sub>2</sub>	0.041	0.072 (+)	0.562
<i>Composite (biomass-related) root traits</i>			
First-order root length	-0.007	0.003 (-)	0.895
Absorptive root length	-0.007	0.003 (-)	0.905
First-order root length density	-0.007	0.003 (-)	0.895
Absorptive root length density	-0.006	0.002 (-)	0.917

895

896

897 **Table 3** Best models (lowest AICc) of stepwise forward multiple regressions between  
 898 plant functional traits and the rhizosphere priming effect. The strength ( $R^2$ ) and  
 899 significance ( $P$ ) of models are displayed.

Model	AICc	Plant functional traits	$R^2$	$P$ -value
1	-44.90	Mean first-order root diameter; Root branching density	0.716	0.043
2	-44.47	Mean first-order root diameter; Root branching density; Root exudate-derived respiration	0.767	0.094
3	-44.31	Mean first-order root diameter	0.607	0.023

900

901

902

903

904

905

906

907

908

909

910

911

912

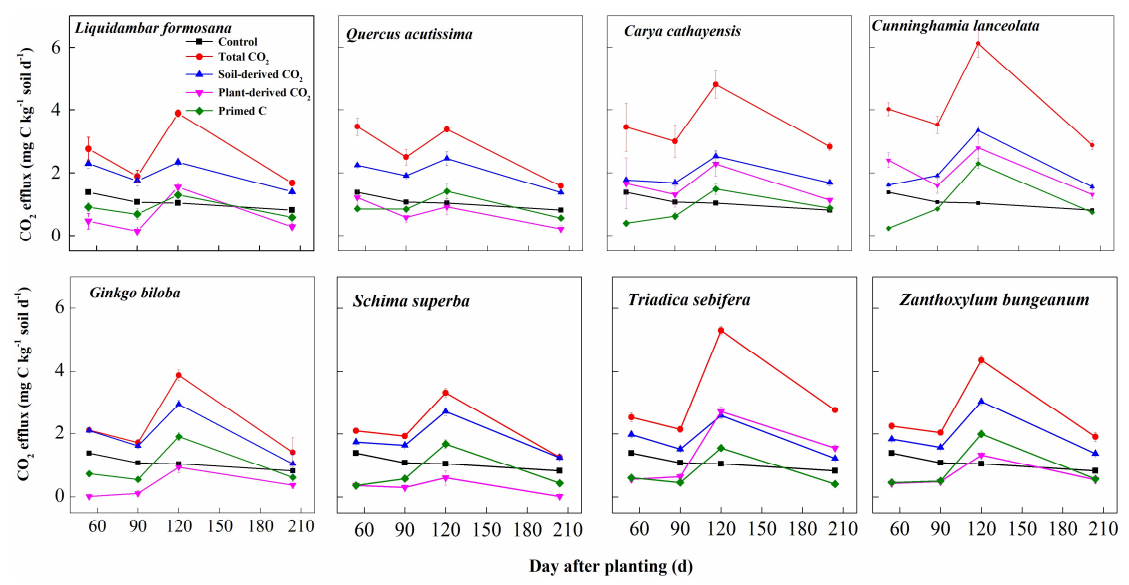
913

914

915

916 **Figure 1**

917



918

919

920

921

922

923

924

925

926

927

928

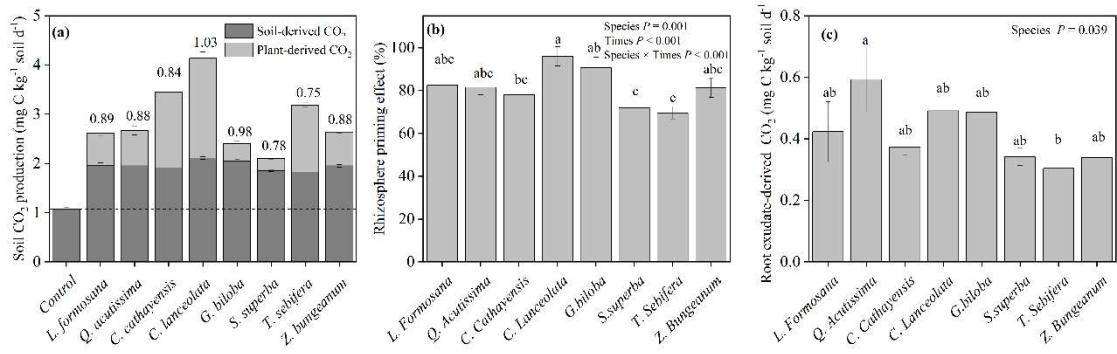
929

930

931

932 **Figure 2**

933



934

935

936

937

938

939

940

941

942

943

944

945

946

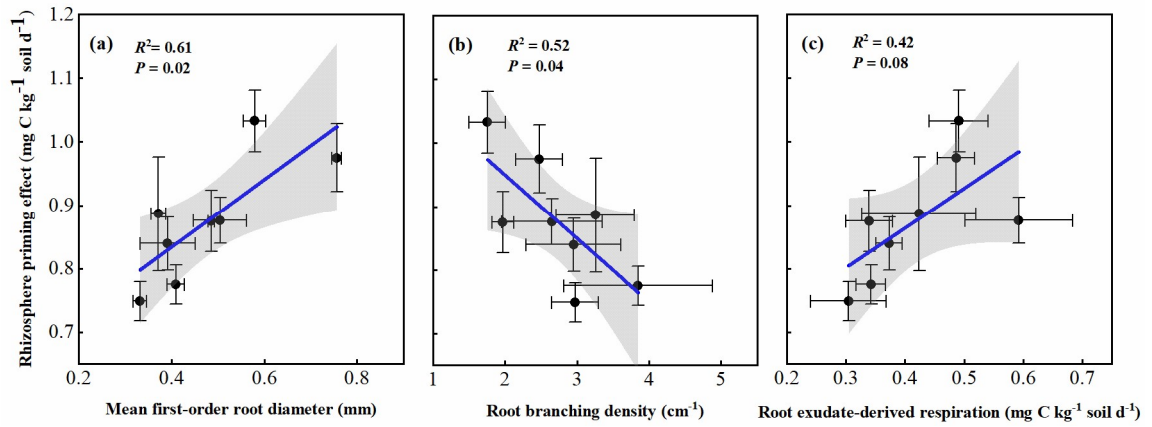
947

948

949

950 **Figure 3**

951



952

953

954

955

956

957

958

959

960

961

962

963

964

965

966

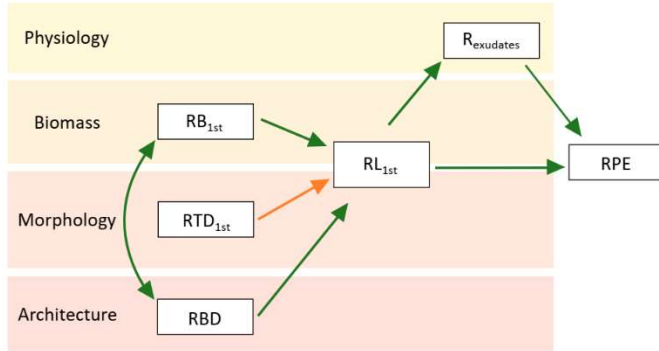
967

968 **Figure 4**

969

**a. Initial (hypothetical) path model**

p-value = 0.000, CFI = 0.609, RMSEA = 0.600, df = 8, AIC = -54.3



970

**b. Final (probable) path models**

p-value = 0.947, CFI = 1.00, RMSEA = 0.000, df = 3, AIC = -58.0

